Available online at www.sciencedirect.com
SCIENCE DIRECT®
Journal of Chromatography A, 1009 (2003) 29–43
JOURNAL OF CHROMATOGRAPHY A
www.elsevier.com/locate/chroma

Temperature profiling of polypeptides in reversed-phase liquid chromatography
I. Monitoring of dimerization and unfolding of amphipathic α-helical peptides

Colin T. Mant[a], Yuxin Chen[b], Robert S. Hodges[a,*]

[a]*Department of Biochemistry and Molecular Genetics, University of Colorado Health Sciences Center, Denver, CO 80262, USA*
[b]*Department of Biochemistry, University of Alberta, Edmonton T6G 2H7, Canada*

Abstract

The present study sets out to extend the utility of reversed-phase liquid chromatography (RP-HPLC) by demonstrating its ability to monitor dimerization and unfolding of de novo designed synthetic amphipathic α-helical peptides on stationary phases of varying hydrophobicity. Thus, we have compared the effect of temperature (5–80 °C) on the RP-HPLC (C_8 or cyano columns) elution behaviour of mixtures of peptides encompassing amphipathic α-helical structure, amphipathic α-helical structure with L- or D-substitutions or non-amphipathic α-helical structure. By comparing the retention behaviour of the helical peptides to a peptide of negligible secondary structure (a random coil), we rationalize that ''temperature profiling'' by RP-HPLC can monitor association of peptide molecules, either through oligomerization or aggregation, or monitor unfolding of α-helical peptides with increasing temperature. We believe that the conformation-dependent response of peptides to RP-HPLC under changing temperature has implications both for general analysis and purification of peptides but also for the de novo design of peptides and proteins.

Keywords: Temperature effects; Polypeptides; Peptides

1. Introduction

One of the most interesting developments of liquid chromatography in recent years has been the emergence of reversed-phase liquid chromatography (RP-HPLC) as a physicochemical probe of peptide and protein structure. Such studies are based on the premise that the hydrophobic interactions between polypeptides and the non-polar stationary phase characteristic of RP-HPLC [1–3] mimic the hydrophobicity and interactions between non-polar residues which are the major driving forces for protein folding and stability. Thus, RP-HPLC has demonstrated its potential for correlating the retention behaviour of peptides [4–17] and proteins with their conformational stability, for monitoring hydrophobicity and amphipathicity of α-helices and β-sheet molecules [3,18–28] and for assessing how the pK_a values of potentially ionizable side-chains, frequently important as enzyme catalytic groups, are influenced by their microenvironment [29]. In addition, we have previously described the design and development of

*Corresponding author. Tel.: +1-303-315-8837; fax: +1-303-315-1153.
E-mail address: robert.hodges@uchsc.edu (R.S. Hodges).

0021-9673/03/$ – see front matter
doi:10.1016/S0021-9673(03)00621-6

a single model ligand–receptor system based on observing the retention behaviour of de novo designed single-stranded amphipathic α-helical peptide ligands binding to a complementary receptor (RP-HPLC stationary phase) [30–32] since hydrophobic interactions play a key role in the binding of ligands to receptors in biological systems.

Much of the efficacy of RP-HPLC as a probe of stability, folding and conformation of peptides and proteins lies in the wealth of stationary phases and/or mobile phase conditions available to the researcher when gauging the potential of relating peptide elution behaviour with structural features (e.g., the amphipathicity of α-helices or cyclic β-sheet peptides; destabilization of conformation) and/or biological activity (e.g., antimicrobial potency, receptor binding). Temperature has also added another dimension to such applications, with physicochemical studies of RP-HPLC of polypeptide solutes under conditions of varying temperature allowing even more insight into conformational stability of peptides and proteins as well as the way such peptidic solutes interact with hydrophobic stationary phases [5,13,33].

The present study sets out to extend the utility of RP-HPLC as an effective physicochemical probe of polypeptide structure by demonstrating its ability to monitor dimerization and unfolding of de novo designed synthetic amphipathic α-helical peptides on stationary phases of varying hydrophobicity when run at temperatures ranging from 5 to 80 °C. Significantly, interactions between non-polar residues, specifically between the non-polar faces of amphipathic α-helical sequences in a protein (50% of α-helices found in proteins are amphipathic) [34,35] are the major driving force for protein folding and stability. In addition, dimerization is a critical factor in explaining biological activity, folding and stability of biological molecules. Thus, we believe that the conformation-dependent response of peptides to RP-HPLC under changing temperature (temperature profiling) has implications, not only for the approach to general analysis and purification of peptides, but also for the de novo design of peptides and proteins, since the contribution of different amino acid side-chains to stability of α-helical structure and oligomerization may be rapidly ascertained through this RP-HPLC approach.

2. Experimental

2.1. Materials

HPLC-grade water was prepared by an E-pure water purification system from Barnstead International (Dubuque, IA, USA). Trifluoroacetic acid (TFA) was obtained from Halocarbon Products (River Edge, NJ, USA). Acetonitrile was obtained from EM Science (Gibbstown, NJ, USA).

2.2. Columns

Analytical RP-HPLC runs were carried out on Zorbax SB300-C_8 and SB300-CN columns (150× 4.6 mm I.D., 5 μm particle size, 300 Å pore size) from Agilent Technologies (Little Falls, DE, USA).

2.3. Instrumentation

RP-HPLC runs were carried out on an Agilent 1100 Series liquid chromatograph.

Peptide synthesis was carried out on an Applied Biosystems peptide synthesizer Model 430A (Foster City, CA, USA).

2.4. Peptide synthesis and purification

Synthesis of the peptides was carried out by standard solid-phase synthesis methodology using *N-tert*.-butyloxycarbonyl (t-Boc) chemistry on co-poly(styrene–1% divinylbenzene) benzhydrylamine resin (0.92 mmol/g resin) as previously described [27] for L-peptide analogues and on MBHA (methylbenzhydrylamine) resin (0.97 mmol/g) as previously described [28] for peptide analogues containing D-amino acids. Crude peptides were purified on an Applied Biosystems 400 solvent-delivery system connected to a 783A programmable absorbance detector or on a Beckman liquid chromatograph using a Zorbax 300 SB-C_8 column (250×9.4 mm I.D., 6.5 μm particle size, 300 Å pore size; Agilent Technologies, Brockville, Canada). Amino acid analyses of purified peptides were carried out on a Beckman Model 6300 amino acid analyzer (Beckman Instruments, Fullerton, CA, USA) and the correct primary ion molecular masses of peptides were confirmed by mass spectrometry on

a Fisons VG Quattro electrospray mass spectrometer (Fisons, Pointe-Claire, Canada).

2.5. Characterization of helical structure

The mean residue molar ellipticities of peptides were determined by circular dichroism spectroscopy, using a Jasco J-720 spectropolarimeter (Jasco, Easton, MD, USA), at 25 °C in the presence of an α-helix inducing solvent, 2,2,2-trifluoroethanol (TFE) (40% TFE in 0.1% aq. TFA, pH 2.0).

2.6. Temperature denaturation

Each peptide was dissolved in 0.1% aq. TFA containing 40% TFE, pH 2.0, to give a peptide concentration of about 0.5 mg/ml. Each solution was loaded into a 0.02 cm fused-silica cell and its ellipticity at 222 nm was measured at different temperatures. The ratio of the molar ellipticity at a particular temperature (t) relative to that at 5 °C $([\theta]_t - [\theta]_u)/([\theta]_5 - [\theta]_u)$ was calculated and plotted against the temperature in order to obtain the thermal melting profiles, where $[\theta]_5$ and $[\theta]_u$ represent the ellipticity values for the fully folded and fully unfolded species, respectively. The melting temperature, T_m, was calculated as the temperature at which the helix was 50% denatured $\{([\theta]_t - [\theta]_u)/([\theta]_5 - [\theta]_u) = 0.5\}$ and the values taken as a measurement of α-helix stability.

3. Results

3.1. Synthetic model peptides used in this study

Table 1 shows the sequence of the synthetic model peptides employed for the present study, these peptides divided generally into three groups: (1) amphipathic α-helical peptides; (2) non-amphipathic α-helical peptides; and (3) a peptide internal standard (C1) with negligible secondary structure (random coil). Fig. 1 shows representations of selected peptides from Table 1 as α-helical nets.

From Fig. 1, peptides LL9 and AA9 represent ''native'' model amphipathic α-helical peptides based on the sequence Ac-E*n*EK*nn*KEXEK*nn*K-E*n*EK-amide, where *n* denotes Ala (AX9 peptides) or Leu (LX9 peptides) and X denotes the residue substituted at position 9 of the sequence. Thus, the LL9 ''native'' analogue has Leu substituted at position 9; similarly, the AA9 ''native'' analogue has Ala substituted at position 9. The result of this well-characterized sequence [30–32,36–39], which has a high potential to form α-helical structure, is an amphipathic helix with a wide hydrophobic face (between the solid lines in the helical net representa-

Table 1
Synthetic peptides used in this study

Peptide sequence[a]	Denotion
Amphipathic α-helical peptides[b]	
Ac-ELEKLLKE**L**EKLLKELEK-amide	LL9
Ac-ELEKLLKE**K**EKLLKELEK-amide	LK9
Ac-EAEKAAKE**A**EKAAKEAEK-amide	AA9
Ac-EAEKAAKE**K**EKAAKEAEK-amide	AK9
Amphipathic α-helical peptides with stereoisomeric substitutions[c]	
Ac-EAEKAAKE**A**EKAAKEAEK-amide	A_L
Ac-EAEKAAKE**L**EKAAKEAEK-amide	L_L, L_D
Ac-EAEKAAKE**I**EKAAKEAEK-amide	I_L, I_D
Ac-EAEKAAKE**T**EKAAKEAEK-amide	T_L, T_D
Ac-EAEKAAKE**P**EKAAKEAEK-amide	P_L, P_D
Ac-EAEKAAKE**G**EKAAKEAEK-amide	G
Non-amphipathic α-helical peptides[d]	
Ac-EELKLKLELELKLKLEEK-amide	naL
Ac-EEAKAKAEAEAKAKAEEK-amide	naA
Random coil peptide[e]	
Ac-ELEKGGLEGEKGGKELEK-amide	C1

[a] Peptide sequences are shown using the one-letter code for amino acid residues; Ac denotes N^{α}-acetyl and amide denotes C-terminal amide.

[b] The amphipathic α-helical peptide LL9 has seven Leu residues in the non-polar face (Fig. 1), while AA9 has seven Ala residues in the non-polar face. Bold residues denote differences between peptide sequences, e.g., LL9 and LK9 have a Leu or a Lys residue, respectively, at position 9 of the otherwise identical sequence, while AA9 and AK9 have an Ala or a Lys residue, respectively, at position 9 of the otherwise identical sequence.

[c] Subscript letter denotes L- or D-amino acid substitution at position 9 of the 18-residue sequence of AA9 (Fig. 1), e.g., L_L denotes substitution of L-Leu at position 9, L_D denotes substitution of D-Leu at position 9, etc. Bold residues denote different L- or D-amino acids substituted at position 9 of the otherwise identical sequence.

[d] naL and naA represent non-amphipathic α-helical analogues of LL9 and AA9, respectively, i.e., same amino acid composition but different sequence; hence, ''na'' denotes non-amphipathic.

[e] C1 denotes random coil control peptide 1.

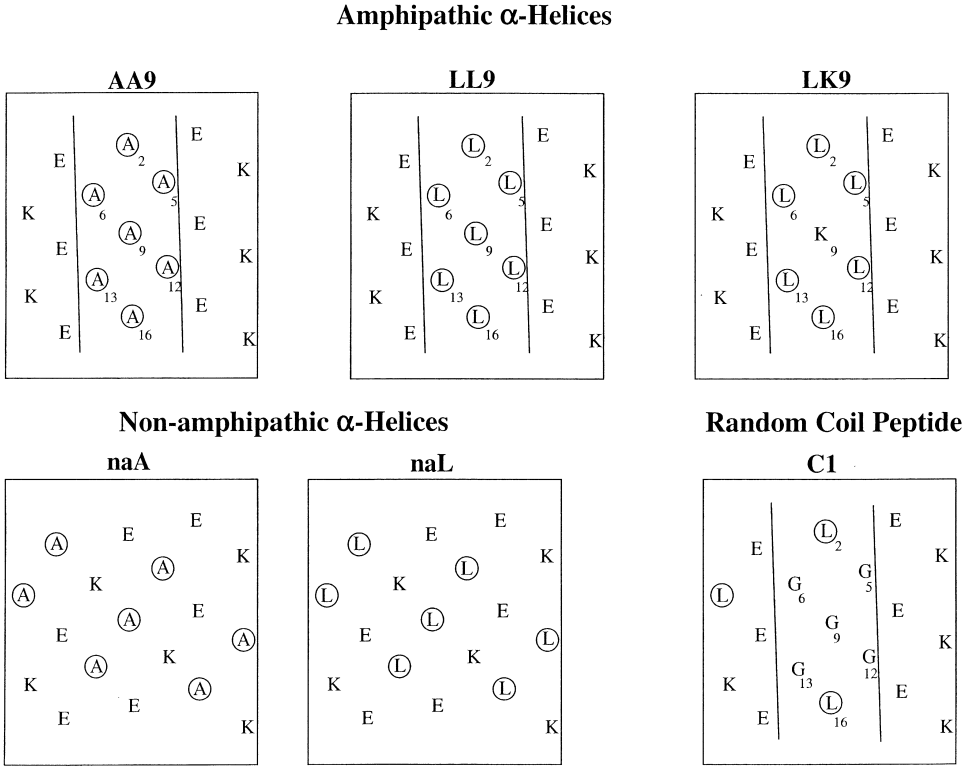

Fig. 1. Representation of synthetic α-helical peptides as α-helical nets. For the ''native'' amphipathic α-helical peptides, LL9 and AA9, the area between the solid lines on the top of the two nets represents the hydrophobic face [made up of Leu (LL9) or Ala (AA9) residues]. The substitution site for peptide analogues (position 9) is in the centre of the non-polar face of these ''native'' peptides, e.g., the analogue with Lys at position 9 is denoted LK9. For the non-amphipathic α-helical peptides, naA and naL, which represent SCDS (same composition, different sequence analogues) of AA9 and LL9, respectively, the distribution of the Ala (naA) or Leu (naL) residues results in non-amphipathic structures. A random coil standard, C1, is also presented as an α-helical net, in order to illustrate the unlikelihood (with several helix-disrupting Gly residues in close proximity in such a conformation) of such secondary structure.

tions of LL9 and AA9; Fig. 1) made up of non-polar residues at positions 2, 5, 6, 9, 12, 13 and 16; the hydrophilic face is made up of Lys and Glu residues. In addition, the LL9 and AA9 peptides are amphipathic α-helical peptides with non-polar faces representing hydrophobic domains of very different hydrophobicities, i.e., a very hydrophobic environment represented by the Leu residues of LL9 and a much less hydrophobic environment created by the Ala residues of AA9. From Fig. 1 and Table 1, LK9, with Lys substituted at position 9 of the LX9 peptides, represents an amphipathic α-helical peptide analogue with a highly hydrophilic, positively charged residue situated in the centre of a very hydrophobic environment; similarly, AK9, with Lys substituted at position 9 of the AX9 peptides, represents an amphipathic α-helical peptide with this positively charged residue situated in the centre of only a moderately hydrophobic environment.

From Table 1, the peptides denoted with subscript L or D refer to the L- or D-amino acid substitutions in the centre of the non-polar face of the AX9 peptide sequence. Thus, A_L denotes the analogue with L-Ala substituted at position 9 of the sequence (identical to AA9), L_D denotes the analogue with D-Leu substituted at position 9 of AX9, etc.

From Table 1 and Fig. 1, the peptides denoted naL and naA represent SCDS (same composition, different sequence) analogues of LL9 and AA9, respectively. As shown in the helical net representations

(Fig. 1), the distribution of the Leu (naL) or Ala (naA) residues results in non-amphipathic structures (hence, ''na'', which denotes non-amphipathic).

Finally, peptide C1 represents a peptide designed to exhibit negligible secondary structure, i.e., a random coil. This peptide was designed to be of similar length and composition to AA9, as well as retention time of similar magnitude to that of AA9. While AA9 contains seven Ala residues, C1 contains none. Instead, five Gly residues and two Leu residues are present in the C1 preferred binding domain if it were α-helical. Thus, with seven Ala residues in AA9 (hence seven CH_3 groups) and five Gly and three Leu residues in C1 (hence twelve CH_2 and CH_3 groups, from the three Leu residues), overall hydrophobicity is essentially maintained. The additional Leu is required to increase the retention time of the random coil peptide to a value similar to that of AA9 with the preferred binding domain. The positioning of the three Leu residues was designed to ensure that they could not form an amphipathic α-helix and, hence, override the destabilizing effect of the Gly residues. From Fig. 1, it can be seen that, even if this peptide was able to be induced into α-helical structure, a non-amphipathic helix would result. However, the presence of five Gly residues (Gly is a known α-helix disrupter and the amino acid with the lowest helical propensity [38,39]) in place of five Ala residues (Ala being the amino acid with highest helical propensity [38,39]) was designed to make any secondary structure highly unlikely to occur.

Illustration of the strong α-helicity of LK9 ($[\theta]_{222}=-28\,450°$) and LL9 ($[\theta]_{222}=-24\,900°$) in the presence of the α-helix-inducing solvent TFE [40–43] at pH 2.0 (50% TFE in 0.1% aq. TFA) is shown in Fig. 2. The high helicity of the amphipathic peptide series in the presence of TFE, of which AA9 is the ''native'' analogue, has been well documented [36,38,39]. In addition, the non-amphipathic analogue of AA9, i.e., naA, has also been shown previously to exhibit strong helicity in the presence of 50% TFE [44], as does the LL9 non-amphipathic analogue, naL, in the present study (data not shown). Since TFE is recognized as a useful mimic of the non-polar environment characteristic of RP-HPLC [8], as well as being a strong α-helix inducer in potentially helical molecules [40–43], elution of these peptide analogues as α-helices during RP-HPLC is ensured. In contrast, from Fig. 2, the peptide designed as a random coil standard, C1, clearly exhibits negligible secondary structure, even in the presence of 50% TFE and at the low temperature of 5 °C ($[\theta]_{222}=-3950°$). Finally, it has also been previously demonstrated that the L- and D-peptide analogues (with the exception of P_L and P_D) all exhibit high α-helical content in the presence of 50% TFE [28].

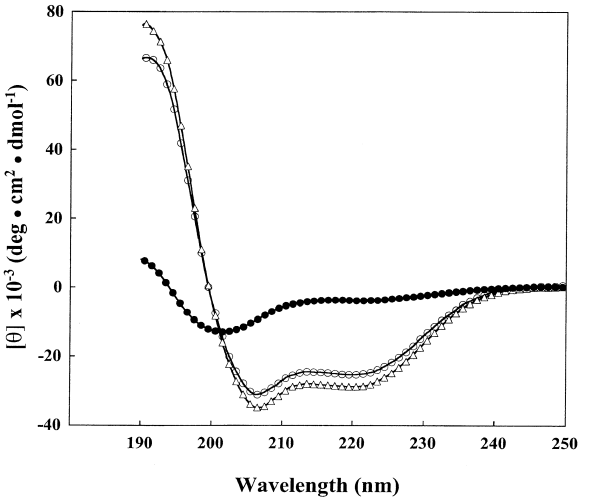

Fig. 2. Circular dichroism spectra of synthetic peptide analogues. The spectra were measured in 40% TFE in 0.1% aq. TFA, pH 2.0. The sequences and nomenclature of the peptides are defined in Table 1. Peptide C1 (●), LL9 (○) and LK9 (△).

3.2. Retention behaviour of model peptides during RP-HPLC

It is well known that the chromatography conditions of RP-HPLC (hydrophobic stationary phase, non-polar eluting solvent) induce and stabilize helical structure in potentially helical polypeptides [8,13,17] in a manner similar to that of the helix-inducing solvent TFE. Polypeptides which are thus induced into an amphipathic α-helix on interaction with a hydrophobic RP-HPLC stationary phase will exhibit preferred binding of their non-polar face with the stationary phase [8]. Fig. 3 shows the RP-HPLC elution profile of α-helical peptides on the C_8 column. From Fig. 3, for peptide pairs AA9/naA and

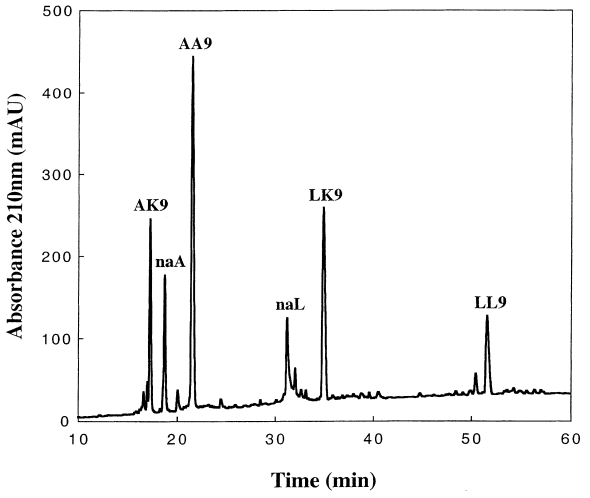

Fig. 3. RP-HPLC of synthetic amphipathic and non-amphipathic α-helical peptides. Column: Zorbax SB300-C_8 (see Experimental). Conditions: linear A–B gradient (1% B/min) at a flow-rate of 0.25 ml/min, where eluent A is 0.05% aq. trifluoroacetic acid (TFA) and eluent B is 0.05% TFA in acetonitrile; temperature, 40 °C. The structures of the amphipathic (AA9, AK9, LL9, LK9) and non-amphipathic (naA, naL) α-helical peptides are shown and defined in Table 1, with helical net representations of AA9, LL9, LK9, naA and naL also shown in Fig. 1.

LL9/naL, the amphipathic analogues (AA9 and LL9) were eluted later than their non-amphipathic analogues (naA and naL, respectively), due to the preferred binding domains (i.e., the non-polar faces) of AA9 and LL9. In addition, the retention times of naL and LL9 are greater compared to naA and AA9, respectively, due to the considerably greater hydrophobicity of Leu compared to Ala [45,46]. Also from Fig. 3, it is clear that substitution of a positively charged Lys residue into the centre of the non-polar face of an amphipathic α-helical peptide (AK9, LK9) decreases significantly the hydrophobicity of the non-polar face, as evidenced by the reduction in RP-HPLC elution times of AK9 and LK9 compared to AA9 and LL9, respectively. It should be noted that the illustrated RP-HPLC run was carried out at 40 °C due to the relatively poor peak shape of naL at lower temperatures.

Fig. 4B shows the RP-HPLC elution profile of L- and D-peptide pairs on the C_8 column. From Fig. 4B, the D-substituted analogues were eluted faster than their corresponding diastereomers. This decrease in retention times of the D-analogues compared to the

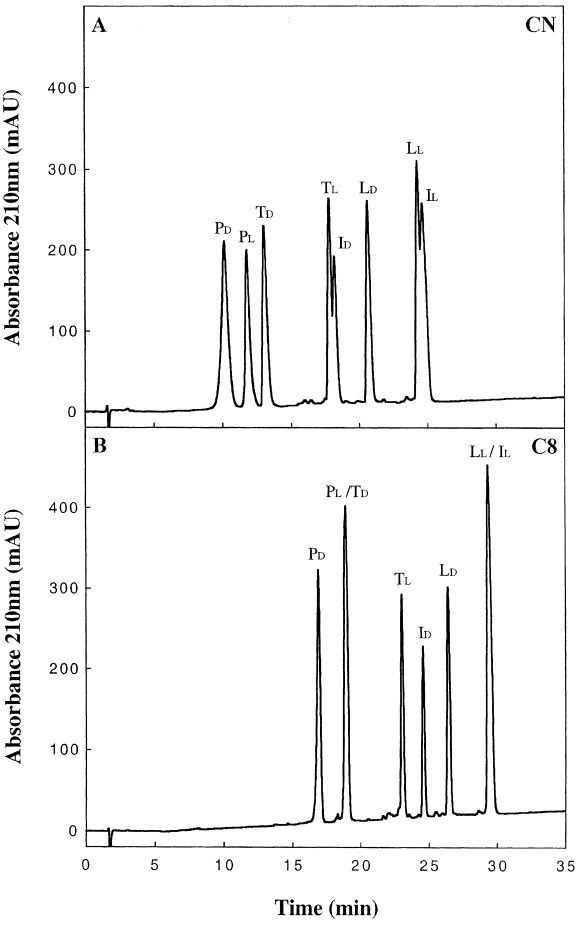

Fig. 4. RP-HPLC of diastereomeric peptide pairs. Columns: Zorbax SB300-C_8 (B) and Zorbax SB300-CN (A) (see Experimental). Conditions: linear A–B gradient (1% B/min) at a flow-rate of 0.25 ml/min, where eluent A is 0.05% aq. TFA and eluent B is 0.05% TFA in acetonitrile; temperature, 25 °C. The structures and descriptions of the peptides are shown in Table 1.

L-analogues can be rationalized as being due to disruption of the hydrophobic face of the amphipathic α-helix due to the introduction of a D-amino acid [10,47–49]. The overall effect would thus be a decrease in the apparent hydrophobicity of the non-polar face of the amphipathic α-helix when substituted with a D-amino acid relative to its L-diastereomer and, hence, a decrease in retention time of the former compared to the latter. Fig. 4A shows the RP-HPLC elution profile of the same peptide mixture on a CN column under the same conditions. Interestingly, peptides co-eluted on the C_8 column

(Fig. 4B) are now completely or partially resolved on the CN column (P_L, T_D and L_L, I_L). Also the retention times of all the peptides are reduced on the CN column (Fig. 4A) relative to the C_8 column, underlining the lesser hydrophobicity of the cyano-substituted stationary phase compared to the C_8 column matrix.

It is important to note that the SB300-C_8 and SB300-CN columns (with SB denoting StableBond) were chosen for this study due to their excellent temperature stability at low pH values [50–52].

3.3. Effect of temperature on RP-HPLC of α-helical peptides

Fig. 5 illustrates the effect of temperature on the retention behaviour of peptides at varying conformation, amphipathicity and stability by presenting the elution profile of a six-peptide mixture at 5 °C (top), 45 °C (middle) and 80 °C (bottom). The profile at 5 °C again shows the effect of amphipathic (AA9) versus non-amphipathic (naA) helical peptide retention behaviour (i.e., AA9 is eluted later than its non-amphipathic homologue, naA) as well as the effect of substituting a positively charged residue (Lys) in the centre of a non-polar face of an amphipathic peptide (i.e., LL9 and AA9 are eluted later than their Lys-substituted counterparts LK9 and AK9, respectively). Of particular note is the elution position of the random coil C1 peptide, whose overall hydrophobicity is clearly similar to that of the apparent hydrophobicities of the AX9 peptides (‘‘apparent’’ due to the preferred binding of the non-polar face of such peptides to the RP-HPLC stationary phase), an important consideration when subsequently attempting to distinguish between the RP-HPLC elution behaviour of amphipathic α-helical peptides versus random coil peptides as the temperature is increased.

At 45 °C (Fig. 5, middle), all peptides, with the exception of LL9, have decreased in retention relative to 5 °C (Fig. 5, top) albeit to differing extents and, thus, leading to a selectivity change in the elution profile which is particularly evident in the separation of the first four eluted peptides (AK9, naA, C1, AA9). In contrast to the other five peptides, the retention time of LL9 has increased at 45 °C compared to 5 °C. Finally, at 80 °C (Fig. 5, bottom),

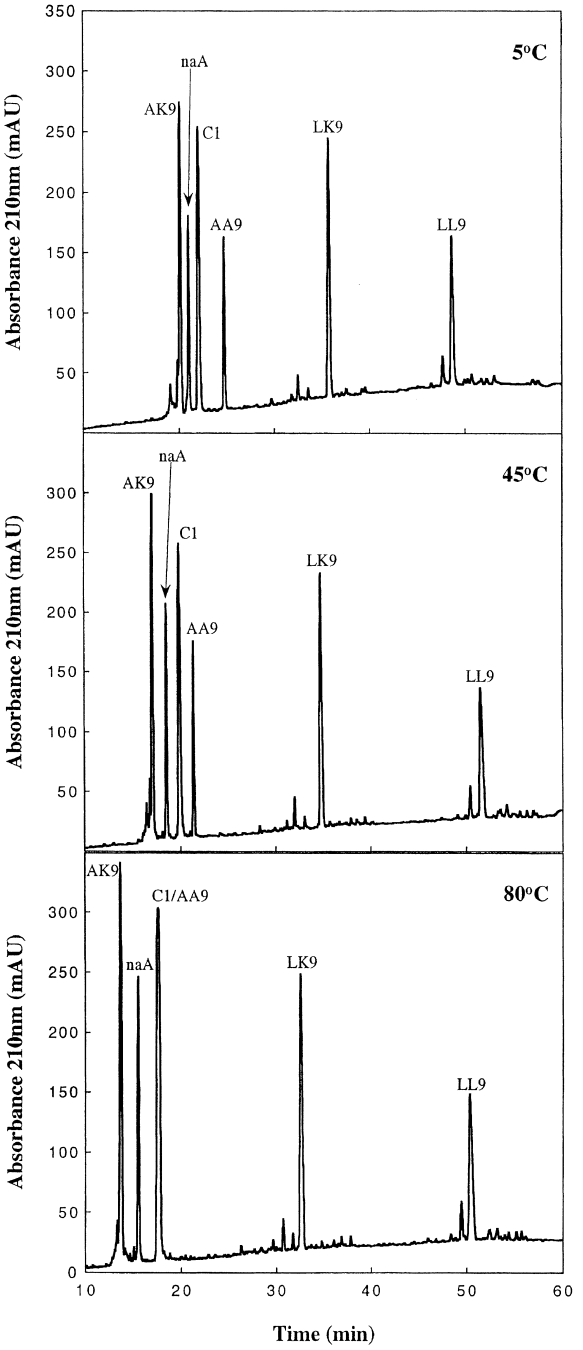

Fig. 5. RP-HPLC of α-helical peptides at 5 °C (top), 45 °C (middle) and 80 °C (bottom). Column: Zorbax SB300-C_8 (see Experimental). Conditions: linear A–B gradient (1% B/min) at a flow-rate of 0.25 ml/min, where eluent A is 0.05% aq. TFA and eluent B is 0.05% TFA in acetonitrile. Peptide structures and descriptions are shown in Table 1.

the retention times of all six peptides have decreased relative to 45 °C (Fig. 5, middle). In addition, selectivity changes effected by this high temperature relative to 45 °C (Fig. 5, middle) and 5 °C (Fig. 5, top) are again clearly apparent for the first four peptides eluted, particularly evident by the co-elution of the amphipathic α-helical AA9 and the random coil C1.

Fig. 6 illustrates the overall effect of temperature on the RP-HPLC elution behaviour of α-helical peptides on the C_8 column. The data are reported as peptide retention time at a particular temperature (t_R) minus its retention time at 5 °C (t_R 5 °C; panel A) or 80 °C (t_R 80 °C; panel B) versus temperature in order to highlight differences in the elution behaviour of peptides as the temperature is raised. From Fig. 6, it is clear that peptides of different amphipathicity/hydrophobicity and conformation behave quite differently during RP-HPLC at different temperatures, although all (with the sole exception of LL9) decrease in retention time relative to the value at 5 °C with increasing temperature (panel A), or (again with the exception of LL9) increase in retention time relative to the value at 80 °C with decreasing temperature (panel B).

The random coil peptide (C1) was included in peptide mixtures to correct for effects of temperature on peptide solubility, mobile phase viscosity and mass transfer, etc., hence assuring that only effects on secondary and tertiary/quaternary structure were being observed. Thus, conclusions concerning the effect on peptide conformation of raising the temperature may be made based on comparing the temperature profiles of the α-helical peptides to that of the random coil peptide standard. From Fig. 6A, the rate of decrease of retention time of naL and LK9 as the temperature is raised incrementally from 5 to 80 °C is less rapid than for the random coil C1. In contrast, the rate of change for naA, AA9 and AK9 is more rapid than that of C1. Finally, the retention behaviour of LL9 is unique in this peptide mixture in that its retention time increases with increasing temperature (up to ~50 °C) and then decreases once more with a further temperature increase. From Fig. 6B, the rate of increase of retention time of naL and LK9 as the temperature is lowered incrementally from 80 to 5 °C is less rapid than for the random coil C1. However, the rate of change for naA, AA9 and AK9 is more rapid than that of C1. Finally, the retention time of LL9 increases up to ~50 °C with decreasing temperature and then decreases once more with a further temperature decrease.

Fig. 7 illustrates the effect of temperature on the RP-HPLC elution behaviour of monomeric α-helical

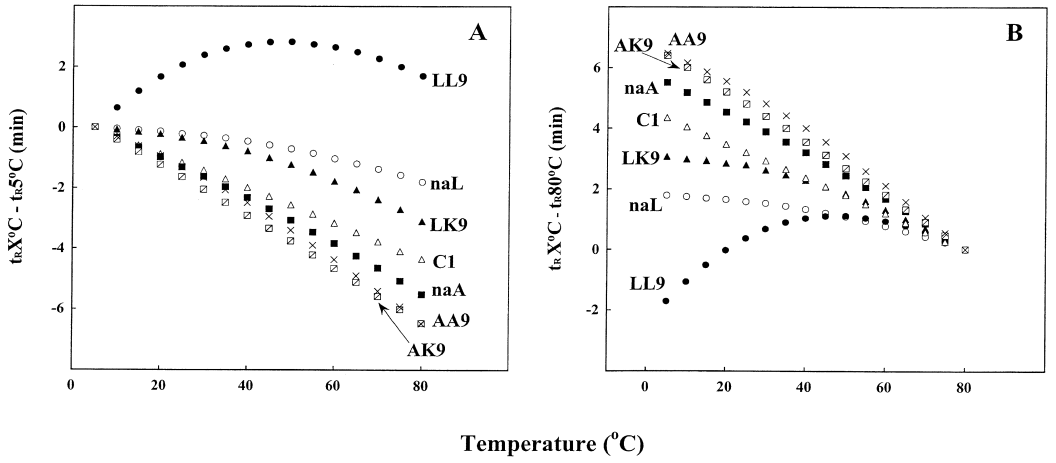

Fig. 6. Effect of temperature on RP-HPLC of α-helical peptides. Column: Zorbax SB300-C_8 (see Experimental). Conditions: linear A–B gradient (1% B/min) at a flow-rate of 0.25 ml/min, where eluent A is 0.05% aq. TFA and eluent B is 0.05% TFA in acetonitrile; temperature, 5–80 °C in 5 °C increments. (A) Temperature against peptide retention time at a specific temperature minus its retention time at 5 °C ($t_R - t_R$ 5 °C). (B) Temperature against peptide retention time at a specific temperature minus its retention time at 80 °C ($t_R - t_R$ 80 °C). Peptide structures and descriptions are shown in Table 1.

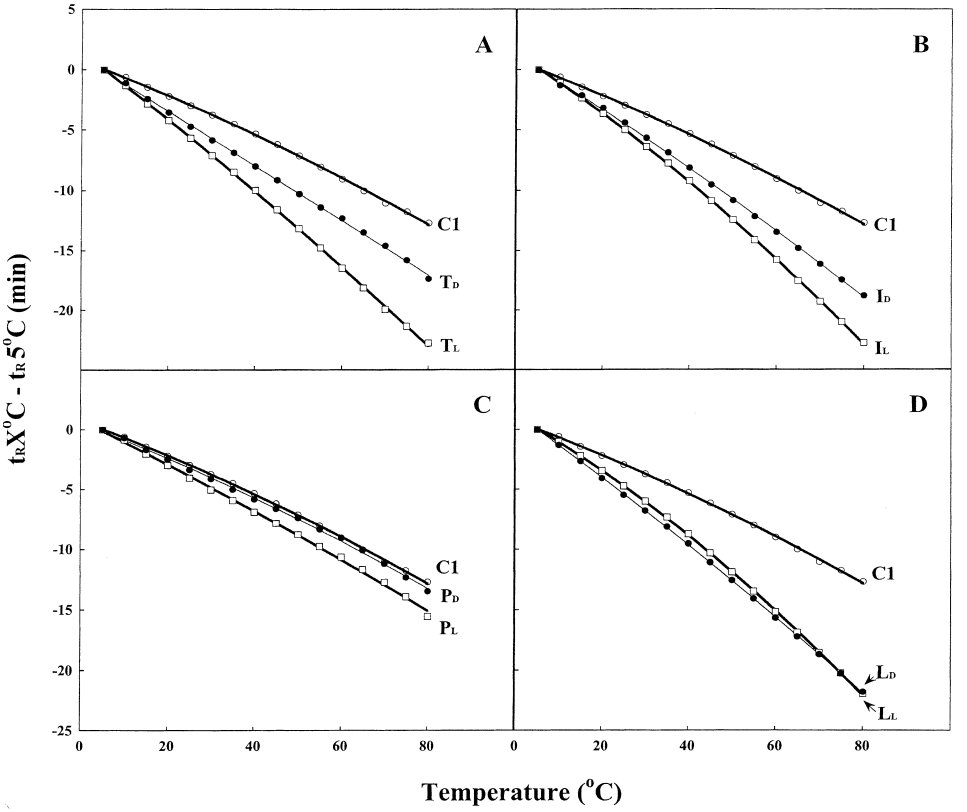

Fig. 7. Effect of temperature on RP-HPLC of L- and D-diastereomeric α-helical peptides. Column: Zorbax SB300-CN (see Experimental). Conditions: linear A–B gradient (0.5% B/min) at a flow-rate of 0.25 ml/min, where eluent A is 0.05% aq. TFA and eluent B is 0.05% TFA in acetonitrile; temperature, 5–80 °C in 5 °C increments. (A–D) Peptide retention time at a specific temperature minus its retention time at 5 °C ($t_R - t_R$ 5 °C) for diastereomeric peptide pairs of Thr-, Ile-, Pro- and Leu-substituted analogues, respectively. The random coil peptide C1 was also included in all runs. Peptide structures and descriptions are shown in Table 1.

diastereomeric peptide pairs on the cyano column. The column was chosen over the considerably more hydrophobic C_8 column [53] since it was hoped that the lesser hydrophobicity, although of a great enough magnitude to induce and/or stabilize α-helical structure when the peptide is bound to the stationary phase, would help not only to allow maximum detection of unfolding of α-helical peptides in solution but also highlight any differences in profiling behaviour between L- and D-peptide pairs. From Fig. 7A–D, in a similar manner to AK9 and AA9 on the C_8 column (Fig. 6), the rate of change in retention behaviour from 5 to 80 °C is faster for all L- and D-peptide pairs compared to the random coil C1. Finally, from Fig. 8, it is interesting to note that a comparison of the effect of temperature on RP-HPLC of several monomeric amphipathic α-helices, all with L-amino acid substitutions at the centre of the non-polar face (L_L, I_L, A_L and G) revealed similar RP-HPLC temperature profiles for all the peptides.

4. Discussion

4.1. Hypothesis for monitoring dimerization and unfolding of α-helical peptides by temperature profiling in RP-HPLC

Although peptides are eluted from a reversed-phase column mainly by an adsorption/desorption mechanism [1,3], even a peptide strongly bound to a

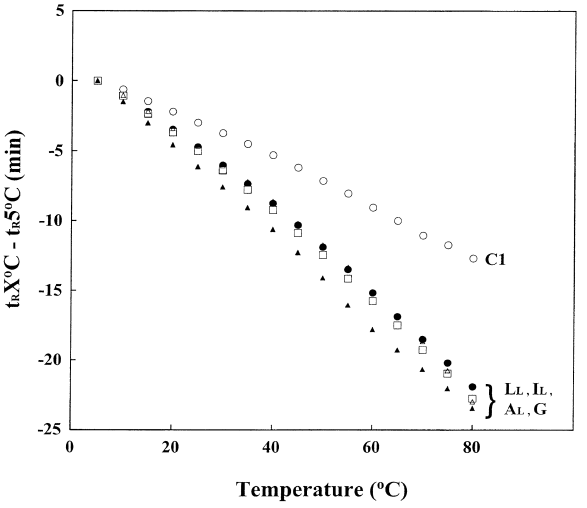

Fig. 8. Effect of temperature on RP-HPLC of monomeric α-helical peptides. Column and conditions: see Fig. 7. The effect of temperature on peptide retention behaviour is plotted as peptide retention time at a specific temperature minus its retention time at 5 °C. Peptide structures and descriptions of the L-substituted Leu-, Ile-, and Ala-substituted analogues (•, □, △, as well as those of the Gly-substituted analogue (▲) and the random coil peptide (C1) (○) are shown in Table 1.

hydrophobic stationary phase will partition between the aqueous mobile phase in equilibrium with its bound state in a narrow range of acetonitrile concentrations during gradient elution.

From Fig. 9 (top) our hypothesis for monitoring peptide dimerization by temperature profiling during RP-HPLC within the small partitioning ''window'' characteristic of peptides [54] is based on four criteria: (1) at low temperature, an amphipathic α-helical peptide able to dimerize in aqueous solution (i.e., associate through its hydrophobic, non-polar face) will dimerize in solution during partitioning, i.e., the concentration of monomer in solution is low and dimer concentration is high; (2) at higher temperatures, the monomer–dimer equilibrium favours the monomer as the dimer is disrupted, thus increasing the concentration of monomer and decreasing the concentration of dimer in solution; (3) at high temperatures, only monomer is present in solution; and (4) whether in the monomeric or dimeric form in solution, the peptide is always bound in its monomeric helical form to the hydrophobic stationary phase. Disruption of the dimer is required for rebinding of the non-polar face of the amphipathic peptide. Thus, the rate of rebinding is faster at lower dimer concentration.

From Fig. 9 (bottom), our hypothesis for monitoring peptide unfolding during RP-HPLC by temperature profiling is based on three criteria: (1) at low temperature, an α-helical peptide is fully folded in solution; (2) as the temperature increases, there is a gradual shift in equilibrium from α-helix to random coil as the peptide unfolds; and (3) at high temperature, whether the peptide is in its monomeric α-helical form or in an unstructured, random coil form in solution, the peptide is always bound to the hydrophobic stationary phase in its monomeric α-helical form.

4.2. Monitoring dimerization and unfolding of α-helical peptides during RP-HPLC

The retention behaviour of LL9, containing a highly hydrophobic non-polar face, suggests dimerization at low temperature with concomitant shielding of the non-polar face of the peptide. As the temperature is raised, there is disruption of dimerization, exposing more of the hydrophobic face of the peptide and, thus, switching the dimer↔monomer equilibrium to more monomeric α-helix at higher temperatures. In addition, the temperature at the maximum Δt_R ($t_R - t_R$ 5 °C) value for LL9 may represent the stability of the dimer under the conditions of chromatography. Interestingly, the helicity of LL9 in the presence of 40% TFE decreased to a small extent ($[\theta]_{222} = -24\,900$ °) compared to its helicity in its absence (−27 300 °), the only analogue to exhibit this result. TFE disrupts tertiary and quaternary structure whilst promoting/maximizing helical structure. Thus, it is possible that, in the absence of TFE, there was interaction between the hydrophobic faces of two LL9 molecules (i.e., dimerization) which also helped to stabilize LL9 helical structure in the absence of a helix-inducing environment. Such helix–helix interaction would subsequently be disrupted in the presence of TFE (as well as by the combined effect of a rise in temperature and the hydrophobic environment of RP-HPLC) even while α-helicity was maintained.

Although LL9 represents the analogue exhibiting the most dramatic effects on retention time of

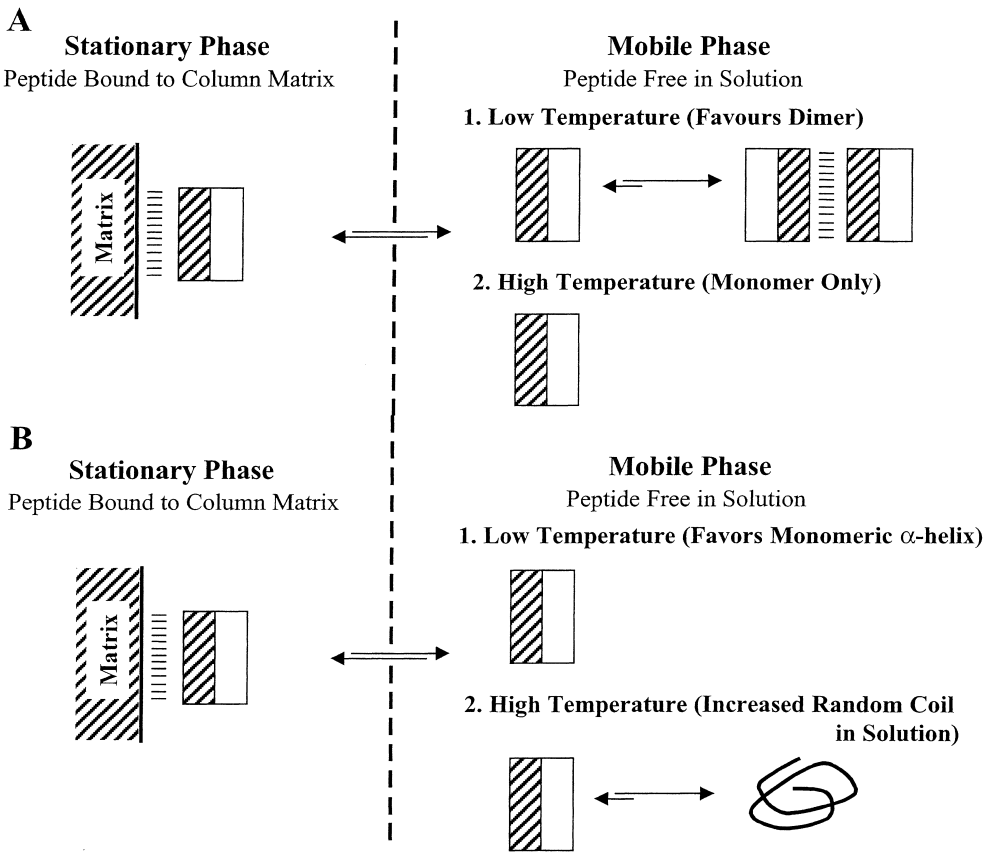

Fig. 9. Top: Hypothesis for monitoring peptide dimerization by temperature profiling in RP-HPLC. Bottom: Hypothesis for monitoring unfolding of monomeric α-helices by temperature profiling in RP-HPLC.

temperature variation, which we speculate as being due to dimerization at lower temperatures, the possibility that other analogues may exhibit a degree of oligomerization was investigated by comparing the temperature profiles of these peptides with that of the random coil standard, C1. Thus, the data from Fig. 6A were now normalized relative to the temperature profile of the random coil standard, the results of which are presented in Fig. 10. From Fig. 10, the positive profile of LL9 suggests little or no unfolding of this very stable peptide (T_m=67.6 °C), even at higher temperatures. Interestingly, the positive profiles of naL and LK9 (Fig. 10) also indicate some association of these molecules at lower temperatures. Significantly, naL exhibited poor peak shape during RP-HPLC at low temperatures, as well as poor solubility in 100% aqueous solution, indicating a tendency to aggregate at low temperature and in the absence of organic modifier. Thus, the positive profile for naL shown in Fig. 10A may indeed be indicative of association (in this case, aggregation) of naL molecules. Concerning LK9, despite its lesser amphipathicity compared to LL9 (due to the presence of the positively charged Lys residue in the centre of the non-polar face of the helix), a combination of the high hydrophobicity of the remainder of the wide non-polar face, still containing six Leu residues (Fig. 1), and the good stability of LK9 (T_m=30.7 °C) may well result in some dimerization at low temperatures. Indeed, it is perhaps a testament to the sensitivity of this profiling approach that such lesser levels of dimerization may be detected. Finally, the negative profiles of the least stable AA9 and AK9 analogues (T_m values of just 17.0 and 17.2 °C,

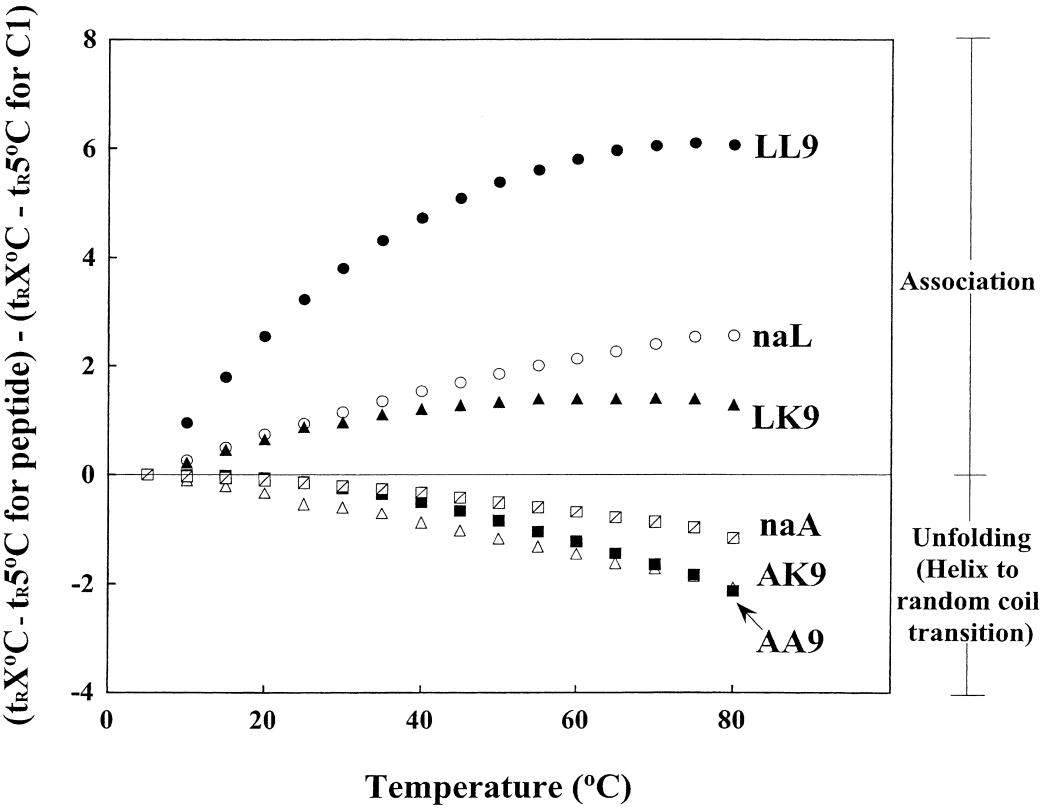

Fig. 10. Effect of temperature on RP-HPLC of α-helical peptides: normalization to retention behaviour of random coil peptide. Column and conditions: see Fig. 5. The retention behaviour of the peptides was normalized to that of random coil peptide C1 through the expression ($t_R - t_R$ 5 °C) minus (t_R C1 $- t_R$ C1 at 5 °C), where t_R and t_R C1 are the retention times at a specific temperature of a helical peptide and the random coil peptide, respectively, and t_R 5 °C and t_R C1 at 5 °C are the retention times at 5 °C. Peptide structures and descriptions are shown in Table 1.

respectively) in Fig. 10B (derived from the temperature profiles shown in Fig. 6A), arising from the faster rates of change relative to C1 in Fig. 6, suggest considerable unfolding of the α-helices with increasing temperature. Thus, at low temperature, the bound monomeric α-helical AA9 and AK9 are in equilibrium with the same monomeric folded states free in solution. Their retention times, at a given temperature, then depend strictly on the hydrophobicity of the moderately non-polar faces of the helices. At high temperature, a considerable amount of the random, unfolded forms of these peptides is now present in solution and the peptides have lost amphipathicity, i.e., no preferred binding domain of AA9 or the lesser amphipathic AK9 is now present. The fast exchange between folded α-helix and random coil affects the retention time, i.e., the more random coil, the greater the decrease in retention time.

To summarize the results presented in Fig. 10, positive profiles relative to the random coil C1 represent an indication of association of peptide molecules, either through oligomerization (e.g., dimerization of LL9 and LK9) or aggregation (e.g., naL); conversely, negative profiles relative to C1 indicate unfolding of the peptides as the temperature is increased, i.e., a helix to random coil transition for naA, AK9 and AA9. In addition, the profiles shown in Fig. 10 (and, indeed, Fig. 6A from which the Fig. 10 profiles are derived) are representative of the effect of increasing temperature on the fully folded state of the peptides, relative as they are to their

retention times at 5 °C. In contrast, the data shown in Fig. 6B are representative of the effect of decreasing temperature on the dissociated state of the peptides, relative as they are to their retention times at 80 °C.

Factors which influence the rate of unfolding of monomeric α-helical peptides were further clarified through comparison of the temperature profiles of the L- and D-peptide analogue pairs (Fig. 7). For instance, as described above, the rate of change in peptide retention behaviour as the temperature is increased from 5 to 80 °C is faster (that is, the temperature profiles are steeper) for all L- and D-peptide pairs compared to the random coil peptide standard, C1, suggesting a helix→random coil unfolding is occurring in solution during RP-HPLC. The rate of unfolding is apparently slower for D-substituted peptides compared to the corresponding L-diastereomer, likely due to the greater folding of the L-peptides compared to the D-peptides at 5 °C as a result of the α-helix disrupting properties of D-amino acids in an α-helix made up of L-amino acids [47–49]. Thus, in the presence of 50% TFE, the maximum molar ellipticities of L-analogues (excluding P_L) were essentially the same (average $[\theta]_{222} = -27\,150°$), suggesting a fully α-helical structure for each peptide analogue [28]. For example T_L (Fig. 7) is more folded at 5 °C ($[\theta]_{222} = -27\,200°$) than T_D ($[\theta]_{222} = -16\,150°$); thus, more α-helix has to unfold during the helix→random coil transition. In contrast, for T_D, there is less helix to unfold and, therefore, the temperature profile more closely resembles the random coil (C1) profile than the folded T_L.

There are distinct temperature profile differences between the diastereomeric peptide pairs, this difference appearing to depend on the maximum α-helicity of the individual peptides in the helix-inducing 50% TFE. As noted previously, TFE is a useful mimic of hydrophobic stationary phases [8]; thus, the helicity measured in 50% TFE is likely a good measure of the helicity of the peptides when bound to the stationary phase. From Fig. 7A, there is a substantial temperature profile difference between T_L and T_D, reflecting significant molar ellipticity (in 50% TFE) differences of 27 200 and 16 150°, respectively. From Fig. 7B, there is also a substantial (though lesser, relative to the T_L/T_D pair) profile difference between I_L and I_D, reflecting molar ellipticity differences of 26 900 and 22 150°, respectively. Fig. 7C illustrates a yet smaller profile difference between P_L and P_D, reflecting molar ellipticity differences of 14 900 and 8150°, respectively. Significantly, such values indicate that just half of the P_L peptide and only ~one-third of the P_D peptide were induced into α-helix in the presence of 50% TFE, reflecting the helix-disrupting properties of Pro. Thus, large proportions of these peptides are already unstructured prior to raising the temperature, which likely explains the temperature profiles, particularly that of P_D, being closer to that of the random coil C1. Finally, from Fig. 7D, the temperature profiles of L_L and L_D are very similar, reflecting essentially identical molar ellipticity values of 26 800 and 26 900°, respectively, i.e., when there is no difference in helical content, there is no difference in the temperature profile. It should be noted that the β-branch of the D-Ile amino acid is more disruptive to the α-helix than D-Leu (molar ellipticity values for I_D and L_D of 22 150 and 26 900°, respectively) and temperature profiling is able to detect this disruption. Temperature profiling is sensitive to conformational change; thus, if there is no change in conformation over the temperature range 5–80 °C, a random-coil peptide and helical peptide will behave similarly.

Fig. 8 compares the effect of temperature on RP-HPLC of several monomeric amphipathic α-helical peptides, all with L-amino acid substitutions at the centre of the non-polar face (Fig. 1). For peptides L_L, I_L, A_L and G, T_m values (i.e., the temperature required to unfold 50% of the α-helix) have been measured as 82, 77.5, 62.5 and 51.5 °C, respectively, i.e., they show a range of stabilities in solution. However, this stability difference is not reflected in their RP-HPLC temperature profiles (Fig. 8), which are all very similar, i.e., the rate of unfolding of the four peptides is similar. This observation may be rationalized by assuming that, in the bound state, all four peptides are fully induced and stabilized in an α-helical conformation, no matter what their stability in solution.

5. Conclusions

We have compared the effect of temperature on the RP-HPLC elution behaviour of mixtures of peptides encompassing amphipathic α-helical struc-

ture, amphipathic α-helical structure with L- versus D-amino acid substitutions in the centre of the non-polar face, non-amphipathic α-helical structure, or negligible secondary structure. From the observation of the retention behaviour of these model peptides over a wide temperature range, we have been able to make initial conclusions concerning the potential efficacy of ''temperature profiling'' by RP-HPLC to monitor dimerization and/or unfolding of α-helical peptides. It appears that temperature profiling is most appropriate for measuring the ability of molecules to oligomerize and dimerization is related to the stability of the oligomer in solution. The logical extension to the present study was to examine the feasibility of this profiling approach to examine the conformation and stability of polypeptides exhibiting higher levels of protein structure (i.e., tertiary and quaternary structure) and this is the subject of a companion paper [33].

Acknowledgements

The work was supported by an N.I.H. grant to R.S.H. (R01GM61855) and the Canadian Bacterial Diseases Network (R.S.H.).

References

[1] C.T. Mant, R.S. Hodges (Eds.), High-Performance Liquid Chromatography of Peptides and Proteins: Separation, Analysis and Conformation, CRC Press, Boca Raton, FL, 1991.
[2] C.T. Mant, R.S. Hodges, Methods Enzymol. 271 (1996) 3.
[3] C.T. Mant, R.S. Hodges, in: K.M. Gooding, F.E. Regnier (Eds.), HPLC of Biological Macromolecules, Marcel Dekker, New York, 2002, p. 433.
[4] M.L. Heinitz, E. Flanigan, R.C. Orlowski, F.E. Regnier, J. Chromatogr. 443 (1988) 229.
[5] A.W. Purcell, M.I. Aguilar, M.T.W. Hearn, J. Chromatogr. 476 (1989) 125.
[6] D.K. Lork, K.K. Unger, H. Bruckner, M.T. Hearn, J. Chromatogr. 476 (1989) 135.
[7] D.E. Henderson, J.A. Mello, J. Chromatogr. 499 (1990) 79.
[8] N.E. Zhou, C.T. Mant, R.S. Hodges, Peptide Res. 3 (1990) 8.
[9] V. Steiner, M. Schar, K.O. Bornsen, M. Mutter, J. Chromatogr. 586 (1991) 43.
[10] M.I. Aguilar, S. Mougos, J. Boublik, J. Rivier, M.T.W. Hearn, J. Chromatogr. 646 (1993) 53.
[11] A.W. Purcell, M.I. Aguilar, M.T.W. Hearn, J. Chromatogr. A 711 (1995) 61.
[12] A.W. Purcell, M.I. Aguilar, M.T.W. Hearn, J. Chromatogr. A 711 (1995) 71.
[13] A.W. Purcell, M.I. Aguilar, R.E.W. Wettenhall, M.T.W. Hearn, Peptide Res. 8 (1995) 160.
[14] S.E. Blondelle, B. Forood, E. Perez-Paya, R.A. Houghten, Int. J. Biochromatogr. 2 (1996) 133.
[15] E. Lazoura, I. Maidonis, E. Bayer, M.T.W. Hearn, Biophys. J. 72 (1997) 238.
[16] T.-H. Lee, P.E. Thompson, M.T. Hearn, M.I. Aguilar, J. Peptide Res. 49 (1997) 394.
[17] D.L. Steer, P.E. Thompson, S.E. Blondelle, R.A. Houghten, M.I. Aguilar, J. Peptide Res. 51 (1998) 401.
[18] C.T. Mant, N.E. Zhou, R.S. Hodges, J. Chromatogr. 476 (1989) 363.
[19] R. Rosenfeld, K. Benedek, J. Chromatogr. 632 (1993) 29.
[20] K. Benedek, J. Chromatogr. 646 (1993) 91.
[21] R.S. Hodges, B.-Y. Zhu, N.E. Zhou, C.T. Mant, J. Chromatogr. A 676 (1994) 3.
[22] K.L. Richards, M.I. Aguilar, M.T.W. Hearn, J. Chromatogr. A 676 (1994) 676.
[23] Y.B. Yu, K.C. Wagschal, C.T. Mant, R.S. Hodges, J. Chromatogr. A 890 (2000) 81.
[24] C.T. Mant, J.R. Litowski, R.S. Hodges, J. Chromatogr. A 816 (1998) 65.
[25] C.T. Mant, L.H. Kondejewski, R.S. Hodges, J. Chromatogr. A 816 (1998) 79.
[26] L.H. Kondejewski, M. Jelokhani-Niaraki, S.W. Farmer, C.M. Kay, B.D. Sykes, R.E.W. Hancock, R.S. Hodges, J. Biol. Chem. 274 (1999) 13181.
[27] B. Tripet, K. Wagschal, P. Lavigne, C.T. Mant, R.S. Hodges, J. Mol. Biol. 300 (2000) 377.
[28] Y. Chen, C.T. Mant, R.S. Hodges, J. Peptide Res. 59 (2002) 18.
[29] T.J. Sereda, C.T. Mant, A.M. Quinn, R.S. Hodges, J. Chromatogr. 646 (1993) 17.
[30] T.J. Sereda, C.T. Mant, F.D. Sönnichsen, R.S. Hodges, J. Chromatogr. A 676 (1994) 139.
[31] C.T. Mant, R.S. Hodges, J. Chromatogr. A 972 (2002) 45.
[32] C.T. Mant, R.S. Hodges, J. Chromatogr. A 972 (2002) 61.
[33] C.T. Mant, B. Tripet, R.S. Hodges, J. Chromatogr., submitted for publication.
[34] J.L. Cornette, K.B. Cease, H. Margalit, J.L. Spouge, J.A. Berzofsky, C.D. DeLis, J. Mol. Biol. 195 (1987) 659.
[35] J.P. Segrest, H. DeLoof, J.G. Dohlman, C.G. Brouillette, G.M. Anantharamaiah, Proteins Struct. Funct. Genet. 8 (1990) 103.
[36] N.E. Zhou, B.-Y. Zhu, B.D. Sykes, R.S. Hodges, J. Am. Chem. Soc. 114 (1992) 4321.
[37] C.T. Mant, N.E. Zhou, R.S. Hodges, in: R.E. Epand (Ed.), The Amphipathic Helix, CRC Press, Boca Raton, FL, 1993, p. 39.
[38] N.E. Zhou, O.D. Monera, C.M. Kay, R.S. Hodges, Protein Peptide Lett. 1 (1994) 114.
[39] O.D. Monera, T.J. Sereda, N.E. Zhou, C.M. Kay, R.S. Hodges, J. Peptide Sci. 1 (1995) 319.

[40] S.Y.M. Lau, A.K. Taneja, R.S. Hodges, J. Biol. Chem. 259 (1984) 13253.
[41] J.W. Nelson, N.R. Kallenbach, Biochemistry 28 (1989) 5256.
[42] T.M. Cooper, R.W. Woody, Biopolymers 30 (1990) 657.
[43] F.D. Sonnichsen, J.E. Van Eyk, R.S. Hodges, B.D. Sykes, Biochemistry 31 (1992) 8790.
[44] T.J. Sereda, C.T. Mant, R.S. Hodges, J. Chromatogr. A 695 (1995) 205.
[45] D. Guo, C.T. Mant, A.K. Taneja, J.M.R. Parker, R.S. Hodges, J. Chromatogr. 359 (1986) 499.
[46] D. Guo, C.T. Mant, A.K. Taneja, R.S. Hodges, J. Chromatogr. 359 (1986) 519.
[47] S. Rothemund, M. Beyermann, E. Krause, G. Krause, M. Bienert, R.S. Hodges, B.D. Sykes, F.D. Sonnichsen, Biochemistry 34 (1995) 12954.
[48] S. Rothemund, E. Krause, M. Beyermann, M. Dathe, M. Bienert, R.S. Hodges, B.D. Sykes, F.D. Sonnichsen, Peptide Res. 9 (1996) 79.
[49] E. Krause, M. Bienert, P. Schmieder, H. Wenschuh, J. Am. Chem. Soc. 122 (2000) 4865.
[50] B.E. Boyes, D.G. Walker, J. Chromatogr. A 691 (1995) 337.
[51] J.J. Kirkland, J.W. Henderson, J.J. DeStefano, M.A. van Straten, H.A. Claessens, J. Chromatogr. A 762 (1997) 97.
[52] C. McNeff, L. Zigan, K. Johnson, P.W. Carr, A. Wang, A.M. Weber-Main, LC·GC 18 (2000) 514.
[53] N.E. Zhou, C.T. Mant, J.J. Kirkland, R.S. Hodges, J. Chromatogr. 548 (1991) 179.
[54] C.T. Mant, T.W.L. Burke, R.S. Hodges, Chromatographia 24 (1987) 565.